Agricultural and Forest Meteorology 259 (2018) 39–47

Contents lists available at ScienceDirect

Agricultural and Forest Meteorology

journal homepage: www.elsevier.com/locate/agrformet

Relating foliage and crown projective cover in Australian tree stands

Adrian Fisher[a,b,*], Peter Scarth[a,c], John Armston[d,a], Tim Danaher[e,a]

[a] Joint Remote Sensing Research Program, School of Earth and Environmental Sciences, University of Queensland, Brisbane, QLD, 4072, Australia
[b] Centre for Ecosystem Science, School of Biological, Earth and Environmental Sciences, University of New South Wales, Sydney, NSW, 2052, Australia
[c] Remote Sensing Centre, Science Delivery, Department of Environment and Science, 41 Boggo Road, QLD, 4102, Australia
[d] Department of Geographical Sciences, University of Maryland, 2181 Samuel J. LeFrak Hall, 7251 Preinkert Drive, College Park, MD, 20742, USA
[e] Office of Environment and Heritage, Alstonville, NSW, 2477, Australia

ARTICLE INFO

Keywords:
Foliage projective cover
Crown projective cover
Crown cover
Canopy Cover
Vertical canopy cover
Canopy gaps

ABSTRACT

Tree cover is quantified using a variety of structural metrics that relate to canopy density, which are often modelled from remotely sensed data. Comparing different metrics, and maps of such metrics, is difficult due to a poor understanding as to how they relate to each other. Two commonly used metrics in Australia are crown projective cover (CPC) and foliage projective cover (FPC). CPC and FPC are the proportion of ground area covered by the vertical projection of tree crowns, and the foliage of tree crowns, respectively. They are dimensionless proportions that vary between zero and one. The relationship between CPC and FPC is a function of the plant area index (PAI), the foliage clumping factor at a zenith angle of zero, the foliage projection function at a zenith angle of zero, tree stand density, mean crown radii, and the proportion of wood to all canopy elements (α). The non-linear relationship was investigated using a dataset of 745 field sites across Australia, for which 1003 coincident CPC and FPC measurements had been made. As measurements of LAI and the other variables were not available, the parameter k was introduced to simplify the equations, which then had only two unknowns: α and k. Best-fit values of α and k were determined using non-linear weighted least-squares regression across all the field sites. Using these values to predict FPC from CPC, and vice versa, achieved low root mean square errors (0.05-0.07) across the field data. The models allow different mapping products to be compared, and also have the potential to facilitate the derivation of FPC from airborne lidar data when field measurements of FPC are not available for calibration. This was demonstrated using a lidar dataset and 12 coincident field sites, across which FPC was derived from a lidar fractional cover metric with an RMSE of 0.08. Further research is required to investigate the stability of this method across different areas and lidar systems.

1. Introduction

Tree cover can be defined using several different structural metrics, such as canopy cover, crown cover, foliage projective cover (FPC) and leaf area index (LAI). Different metrics are measured for different purposes, and although they can follow standard definitions, little systematic research has been conducted into how they relate to each other in real tree stands. Some researchers have attempted to standardise the terminology (Gonsamo et al., 2013), though confusion is still common. A greater understanding of the relationships between metrics is required, to allow data acquired using different methods to be compared, and to ensure that maps based on different metrics are interpreted correctly. Such a comparison should also provide a greater understanding of the inherent structural properties of trees.

Of the commonly used metrics, crown cover is perhaps the simplest to define. It is the proportion of ground area covered by the vertical projection of tree crowns, which are assumed to be opaque and have no overlaps (Gonsamo et al., 2013; Walker and Hopkins et al., 1990). For the purposes of defining all metrics, we define trees as woody vegetation greater than 2 m in height. Crown cover is relatively easy to measure in the field (Walker and Hopkins et al., 1990) and can be mapped from aerial photography (Fensham et al., 2003). It has been referred to by other names, such as canopy closure, canopy cover, or vertical canopy cover, and is commonly used for forest inventories or in definitions of forest (FAO, 2012). In closed forests, crown cover is the inverse of between-crown gaps, which are often the focus for forest ecology and management (Schliemann and Bockheim, 2011). Some definitions of crown cover include the total area of all tree crowns, counting overlap zones twice (Gonsamo et al., 2013). In order to make the definition used in the present paper clear, we propose a new term:

* Corresponding author at: Joint Remote Sensing Research Program, School of Earth and Environmental Sciences, University of Queensland, Brisbane, QLD, 4072, Australia.
E-mail addresses: adrian.fisher@unsw.edu.au, a.fisher2@uq.edu.au (A. Fisher), p.scarth@uq.edu.au (P. Scarth), armston@umd.edu (J. Armston), tim.danaher@environment.nsw.gov.au (T. Danaher).

https://doi.org/10.1016/j.agrformet.2018.04.016
Received 6 August 2017; Received in revised form 17 April 2018; Accepted 18 April 2018
Available online 26 April 2018
0168-1923/

crown projective cover (CPC). By including the word projective, it is clear that CPC only counts overlaps once, as they project onto the same patch of ground.

FPC is the proportion of ground area covered by the vertical projection of tree crown foliage (Specht, 1983; Walker and Hopkins et al., 1990). It was developed in Australia, where it is commonly used to record the canopy foliage density of native tree stands, which mostly do not seasonally drop leaves. It is typically measured in the field using transects (Johansson, 1985), which requires more time than measuring CPC in order to distinguish the foliage and woody canopy elements and the within-crown gaps. FPC is more closely related to LAI and the photosynthetic and evaporative potential of a plant community than CPC, especially in Australian trees and shrubs, which often have low foliage density (Specht, 1983). While CPC treats crowns as opaque objects, the FPC of individual crowns for most Australian woody plants is between 40% and 70% depending on crown architecture (Walker and Hopkins et al., 1990). This also means that FPC has a higher dynamic range than CPC, which usually reaches 0.951.00 for FPC values in the range 0.751.00 (Scarth et al., 2008; Scarth and Phinn, 2000).

LAI is defined as half the total surface area of green leaves per unit of horizontal ground surface area (Chen and Black, 1992). LAI is the main variable used to model canopy photosynthesis and evapotranspiration, as it determines the size of the plant–atmosphere interface and the exchange of energy and mass between the canopy and the atmosphere (Chen et al., 1997; Simioni et al., 2003). Trees may have similar LAI values and very different FPC values due to variation in foliage clumping and leaf orientation angle (Campbell, 1990; Henry et al., 2002). This difference is pronounced in Australian trees and shrubs, whose leaf orientation angle and foliage clumping can be highly variable (Falster and Westoby, 2003; King, 1997). Furthermore, while LAI can be greater than one for dense foliage with overlapping leaves, FPC saturates at a maximum of one. LAI can be determined through direct measurements after destructive sampling or sometimes through leaf litter collection, but is often estimated through indirect means such as measuring light interception or hemispherical photography (Jonckheere et al., 2004). These indirect methods are measuring the proportion of gaps in the canopy (P_{gap}), from which LAI can be modelled, requiring assumptions about the proportion of canopy elements that are wood or foliage.

LAI and FPC are dynamic measures of foliage density, exhibiting changes due to growth, drought, pests, diseases or fires. They are both sensitive to the number of leaves present, and also to the way leaves are distributed and orientated. While LAI will increase through the seasonal vertical growth of foliage shoots, FPC is less sensitive to these changes and is therefore a less dynamic metric (Specht and Specht, 1999). As Australian soils are often low in plant nutrients, foliation and defoliation tends to be synchronous and FPC remains relatively constant throughout the year (Specht, 1983). Furthermore, it has been shown that FPC of mature vegetation in Australia is correlated to the annual water balance of the ecosystem and remains relatively stable over the long-term (Specht, 1983). Even the dynamic nature of LAI is likely to be reduced in Australia, where very few trees are deciduous, even in the seasonal tropics (Bowman and Prior, 2005). CPC is also relatively stable, increasing slowly with tree growth, and decreasing when branches are lost or trees die.

The research presented here was conducted to investigate the relationship between CPC and FPC in native Australian trees, as these two metrics have been used by different organisations to map and monitor vegetation over large areas. For example, Australia's State of the Forests defined forest as vegetation greater than 2 m in height with a minimum CPC of 20% (Montreal Process Implementation Group for Australia and National Forest Inventory Steering Committee, 2013). Other organisations have used FPC modelled from satellite imagery or airborne lidar to indicate tree cover (Armston et al., 2009; Danaher et al., 2010; Fisher et al., 2016; Lucas et al., 2006; Queensland Department of Science Information Technology Innovation and the Arts, 2014). Rough methods of converting between the metrics are often used, such as the observation that 20% CPC is approximately equivalent to 12% FPC (Henry et al., 2002). It is also possible that developing a model between CPC and FPC will assist with modelling FPC from airborne lidar data, which generally cannot distinguish wood and foliage canopy elements.

The three main objectives were designed to improve our understanding of how FPC and CPC relate to each other. Firstly, the theoretical model describing canopy foliage light interception and the spatial distribution of crowns developed by Nilson (1999) is presented in the context of relating FPC and CPC. Secondly, an extensive dataset of field measured CPC and FPC was used to examine how the theoretical models can be applied to native Australian vegetation. Thirdly, we demonstrate how a greater understanding of the relationship between FPC and CPC can be used in some examples of mapping applications, with particular emphasis on airborne lidar data. The research builds on a previous investigation conducted by Scarth et al. (2008), who examined the nature of the non-linear relationship between CPC and FPC for native vegetation in Queensland with a smaller, preliminary dataset.

2. Theory

Nilson (1999) developed several models for $P_{gap}(\theta)$, the probability of a beam of light travelling through a gap between the canopy of a stand of trees. The simplest model from earlier work by Nilson (1971) is referred to as the exponential model (Eq. (1)).

$$P_{gap}(\theta) = e^{-\frac{G(\theta)\Omega(\theta)\mathrm{PAI}}{\cos(\theta)}} \tag{1}$$

where θ is the zenith angle of the light, PAI is the plant area index, $\Omega(\theta)$ is the stand foliage clumping factor, and $G(\theta)$ is a function describing the area of foliage projected onto a plane perpendicular to θ, which is dependent on the leaf angle distribution. Eq. (1) uses PAI rather than LAI, to account for the proportion of woody elements to all canopy elements (α), where PAI = LAI/(1 − α) (Chen and Cihlar, 1996).

As FPC is dependent on the distribution of the foliage component viewed at a zero zenith angle, it can be modelled as a function of LAI, according to Eq. (2)(Armston et al., 2012).

$$\mathrm{FPC} = 1 - e^{-G(0)\Omega(0)\mathrm{LAI}} \tag{2}$$

Combining Eqs. (1) and (2), allows FPC to be modelled as a function of P_{gap} and α (Eq. (3)), or α as a function of FPC and P_{gap} (Eq. (4)). It is interesting to note that while LAI is a linear function of PAI and α, the relationship between FPC, P_{gap} and α requires a power function to account for the vertical projection.

$$\mathrm{FPC} = 1 - P_{gap}(0)^{1-\alpha} \tag{3}$$

$$\alpha = 1 - \frac{\log(1-\mathrm{FPC})}{\log(P_{gap}(0))} \tag{4}$$

Nilson (1999) found that the simple exponential model in Eq. (1) underestimated $P_{gap}(\theta)$ when compared to that measured by light interception or hemispherical photography, so more complex models were developed incorporating factors relating to the clumping and overlapping of tree crowns, such as the modified Poisson model (Eqs. (5a), (5b), (5c)).

$$P_{gap}(\theta) = e^{\left(\frac{\ln \mathrm{GI}}{1-\mathrm{GI}} CK \left(1 - e^{\left(\frac{-G(\theta)\Omega(\theta)\mathrm{PAI}}{\cos(\theta)CK}\right)}\right)\right)} \tag{5a}$$

where

$$C = \lambda_c \pi r_c^2 \tag{5b}$$

and

$$K = \sqrt{1 + \left(\frac{h}{2r_c}\right)^2 \tan^2\theta} \tag{5c}$$

where λ_c is the tree stand density (trees/m^2), r_c is the mean crown radii (m), h is the crown length (m), and GI is the grouping index, which is related to CPC through Eq. (6). C is the crown closure and K is the relative change of projection area of the crowns, which are assumed to be ellipsoids of rotation.

$$\mathrm{CPC} = 1-e^{\frac{C\ln \mathrm{GI}}{1-\mathrm{GI}}} \tag{6}$$

Combining Eqs. (3), (5a), (5b), (5c) and (6) with a zenith angle of zero eliminates many terms, and results in a model that relates FPC and CPC (Eq. (7)). In order to solve Eq. (7), and calculate FPC from CPC, estimates of α, PAI, $G(0)$, $\Omega(0)$, λ_c and r_c are required. When these values are unknown, it is possible to simplify the relationship between FPC from CPC by replacing $\frac{G(0)\Omega(0)\mathrm{PAI}}{\lambda_c \pi {r_c}^2}$ in Eq. (7) with the empirical parameter k, resulting in Eq. (8). It is also possible to rearrange Eq. (8) to solve for CPC as a function of FPC, k and α (Eq. (9)), or to solve for k as a function of FPC, CPC and α (Eq. (10)).

$$FPC = 1-\left(e^{\log(1-\mathrm{CPC})\left(1-e^{\left(\frac{-G(0)\Omega(0)\mathrm{PAI}}{\lambda_c \pi {r_c}^2}\right)}\right)}\right)^{1-\alpha} \tag{7}$$

$$\mathrm{FPC} = 1-(e^{\log(1-\mathrm{CPC})(1-e^{-k})})^{1-\alpha} \tag{8}$$

$$\mathrm{CPC} = 1-e^{\frac{\log\left((1-\mathrm{FPC})^{\frac{1}{1-\alpha}}\right)}{1-e^{-k}}} \tag{9}$$

$$k = -\log\left(1-\frac{\log\left((1-\mathrm{FPC})^{\frac{1}{1-\alpha}}\right)}{\log(1-\mathrm{CPC})}\right) \tag{10}$$

The models presented in Eqs. (8), (9) and (10) assume that the horizontal distribution pattern of tree crowns in a stand can be described by the Poisson distribution. Nilson (1999) also developed a model where the tree crown pattern was described by the binomial distribution, however, this model has a more complicated form with respect to GI, and is difficult to develop with respect to CPC.

3. Methods

3.1. Study sites

Over the past two decades vegetation structure has been measured in Australia using the star transect method, developed by the Queensland government (Muir et al., 2011). At the time of the analysis presented here, 915 sites with over-storey vegetation had been measured across all of Australia's states and mainland territories, although the majority of sites are in Queensland and the Northern Territory (Fig. 1). As several of the sites have been measured multiple times in order to quantify changes in FPC over time, the number of star transect measurements totals 1190. Of these field measurements 715 are available through the Terrestrial Ecosystem Research Network (TERN) AusCover Remote Sensing Data Facility (Trevithick, 2017), which is a public online spatial database available at http://data.auscover.org.au/Portal2/. The remaining data were collected for restricted use by state and territory government agencies in cooperation with the Joint Remote Sensing Research program (JRSRP) at the University of Queensland.

The site locations were not systematically determined, but represent the opportunistic accumulation from several local, regional and national projects. They cover an enormous range of Australian native vegetation community types across 52 of the 85 Interim Biogeographic Regions of Australia (IBRA), from the tropics in the north through the central deserts to the cool temperate environments in the south. Although several large areas of Australia have not yet been sampled, it represents a remarkable achievement in cooperation, and is set to keep expanding throughout the continent as new sites are measured (Fig. 1).

All the sites contain at least one tree or shrub taller than 2 m, and cover a very wide range in CPC (0.003–1.000) and FPC (0.003–0.960) values. Classifying the sites using the commonly used FPC thresholds of 0.1, 0.3 and 0.7 (Specht, 1970), results in 524 open woodland, 254 woodland, 112 open forest and 25 closed forest sites (Fig. 1). Although vegetation height, stand basal area (SBA) and species were not systematically determined at all sites, the recorded average vegetation height varied from 2-55 m, the recorded SBA varied from 0.1569.14 m^{2}ha^{-1}, and over half of the sites were dominated by Eucalyptus species. Other common species sampled were from the following genera: Acacia, Angophera, Banksia, Brachychiton, Callitris, Casuarina, Corymbia, Flindersia, Grevillea, Hakea, and Melaleuca.

3.2. Transect measurements

At each site the star transect method was used to measure FPC and CPC from 300 vertical tube observations (Muir et al., 2011). This involved three 100 m measuring tapes being laid out at 60° intervals in a star shape, with the centre point located by GPS. Over-storey (woody plants ≥ 2 m height) observations were made at 1 m intervals along each transect using a densitometer (a pole mounted sighting tube with a mirror, a centred cross-hair and two bubble-line levels), and were also classified as either within or between tree crowns, where crown edges were determined as the convex hull surrounding all living crown components (Muir et al., 2011). From the observations recorded at each star transect, P_{gap} was calculated according to Eq. (11), and FPC was calculated according to Eq. (12) (Armston et al., 2009).

$$P_{gap} = 1-(P_{o,g} + P_{o,b}) \tag{11}$$

$$\mathrm{FPC} = \frac{P_{o,g}}{(1-P_{o,b})} \tag{12}$$

where $P_{o,g}$ was the proportion of over-storey green foliage observations, $P_{o,b}$ was the proportion of over-storey branch observations. Eq. (12) assumes that over-storey branch observations are likely to occlude green foliage from the observer. CPC was calculated as the proportion of over-storey observations that were within living tree crowns. Eq. (4) was used to calculate site specific values of α, and Eq. (10) was used to calculate site specific values of k. The CPC of three sites that had values of one were reduced to 0.9999, to allow Eq. (8) to be solved. Also, 187 sites with very low tree cover had incompatible P_{gap}, FPC and CPC values, and were excluded. Thus, of the 1190 site measurements, 1003 (across 745 different sites) were used to conduct the analyses.

Measurement errors from the star transect method are not easily quantified. The measurements have a known bias, with more observations in the centre of the star, and they have a possible observer bias, especially in tall canopies, and on windy days (Trevithick et al., 2012). Also, although the site measurements of FPC and CPC are based on a sample of 300 points, any points between tree crowns do not contribute to the measurement of α. Thus, estimates of α have larger uncertainty for sites where CPC and FPC are low.

3.3. Climate data

Previous work had concluded that sites experiencing drought stress had lower than expected FPC for any given CPC due to fewer leaves reducing the LAI and a steeper mean leaf angle reducing the projection function $G(0)$ (Scarth et al., 2008). To investigate this, climate data processed according to Jones et al. (2009) were downloaded from the Bureau of Meteorology (2015), consisting of Australia-wide, gridded monthly rainfall totals and temperatures (the monthly mean of the daily maximum) from January 1911 until September 2015. These represent a weighted average of recorded weather station data at 0.05° resolution data across the whole of Australia (Jones et al., 2009). Mean annual

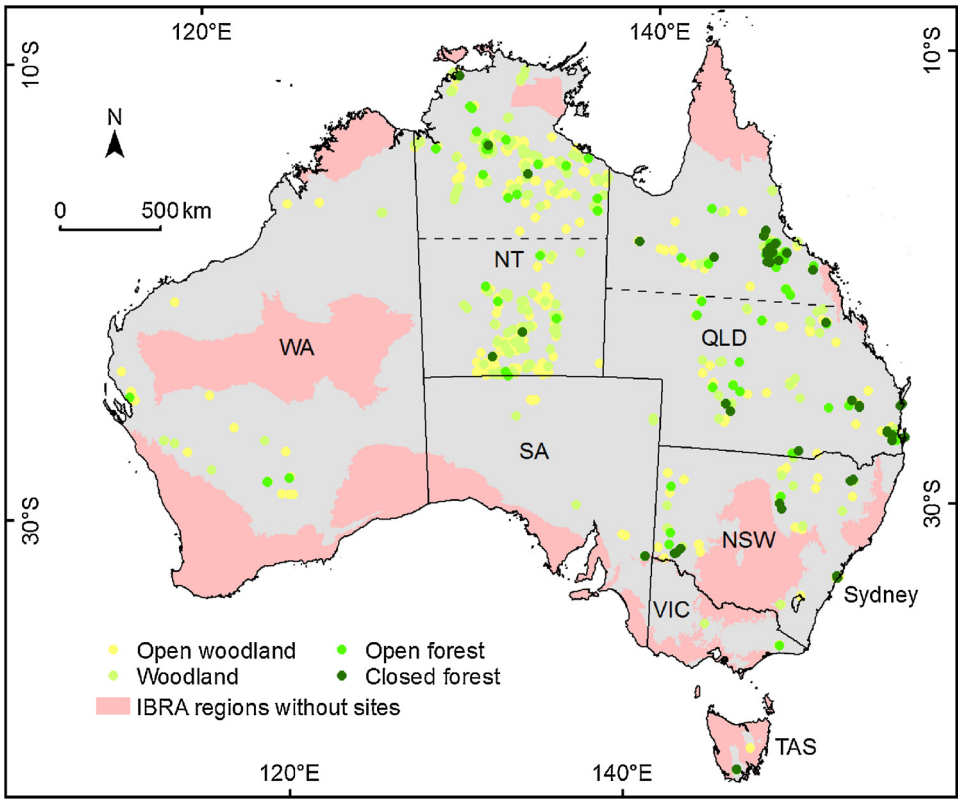

Fig. 1. The 915 transect sites across Australia, classified into open woodland, woodland, open forest and closed forest using the commonly used FPC thresholds of 0.1, 0.3 and 0.7 (Specht, 1970). The sites are distributed over 52 of the 85 Interim Biogeographic Regions of Australia (IBRA), not including small island regions. Labels indicate the states of Queensland (QLD), New South Wales, (NSW), Victoria (VIC), Tasmania (TAS), South Australia (SA) and Western Australia (WA), and the Northern Territory (NT). The dashed lines across the NT and QLD define the north and south divisions used to create Fig. 6.

precipitation and mean daily maximum temperature was also downloaded, to examine the relationship between FPC, CPC and general climatic conditions.

To determine the drought stress at the time and location each of our sites were measured, the Standardized Precipitation and Evapotranspiration Index (SPEI) was calculated from the rainfall and temperature data (Vicente-Serrano et al., 2010). The SPEI is a multi-scalar probabilistic drought index where the precipitation minus potential evapotranspiration (PET) time-series is fitted to a probability distribution, and the variance of each period from the normally distributed probability density is calculated. The SPEI incorporates the influence of rainfall and temperature on droughts, and allows the frequency, magnitude and duration of droughts to be examined at different temporal scales. It was calculated using the freely available SPEI package developed for the R statistical software (R Development Core Team, 2016), which also allowed the calculation of PET from temperature and latitude records using the method of Thornthwaite (1948). We calculated SPEI at two temporal scales of 6 months ($SPEI_6$) and 2 years ($SPEI_{24}$), to examine the effect of short and long-term droughts.

3.4. Analyses

Firstly, the distributions of α and k values were examined, as were the relationships between these and other variables. Secondly, the best fit value of α was determined as that which minimized the root mean square error (RMSE) between measured FPC values and those modelled from P_{gap} using Eq. (3). This was achieved using non-linear weighted least-squares regression, implemented in R (Bates and Watts, 1988; R Development Core Team, 2016). Each site was weighted equally; sites with only one measurement had a weight of 1, while each measurement from a site with n visits had a weighting of $1/n$. Thirdly, the possibility of simplifying Eqs. (8) and (9) to provide a means of predicting FPC from CPC and *vice versa* was assessed. This used non-linear weighted least-squares regression to determine the best fit value of k, for both Eqs. (8) and (9). Fourthly, the relationships between k (calculated from site measurements using Eq. (10)) and site climate variables were examined, to assess whether long term site conditions and short-term drought indices could be used to predict k.

3.5. Application to airborne lidar

Establishing a relationship between field measurements of crown and foliage projective cover has potential to assist in calibrating airborne lidar derived canopy density metrics. Airborne lidar data can provide metrics of canopy density as laser pulses penetrate gaps within and between tree crowns and reflect off foliage and woody elements, as well as the ground (Wulder et al., 2012). Metrics such as the proportion of lidar first returns greater than 2 m above ground are related to FPC, although models are required to remove biases from lidar instrument/survey effects and the ratio of wood to foliage in the canopy (Armston et al., 2009; Ediriweera et al., 2013; Gill et al., 2009). Others have tested methods of modelling CPC from lidar return heights (Chen et al., 2004; Korhonen et al., 2011; Vepakomma et al., 2008). Field data are essential for calibrating these modelling approaches, but as lidar surveys become more common there is a great deal of data available that has been acquired without field campaigns. A method of modelling standardized FPC from airborne lidar derived metrics without calibration against field measurements would be extremely useful. The following sections outline the proposed method, and then describe a dataset of coincident star transects and airborne lidar data that are used to test the method.

3.5.1. Deriving CPC and FPC from airborne lidar

Lidar fractional cover (f), calculated as the proportion of lidar first returns greater than 2 m above ground, is closely related to P_{gap}, CPC and FPC (Lovell et al., 2003). Armston et al. (2009) used f as a proxy for P_{gap}, assuming that the lidar pulses could penetrate between-crown and within-crown gaps, and used Eq. (3) to model FPC for a best fit value of α. Korhonen et al. (2011) found that f was a good proxy for CPC, with an RMSE of 7% across 22 sites. This suggests that in some cases within-

crown gaps are not penetrated by lidar pulses, which is obviously dependant on their size and the lidar pulse footprint diameter. If it is assumed that f is a proxy for CPC, then it is possible to apply Eq. (8) to convert these to FPC values. This requires values for α and k, which can be calculated as the best fit values for the Australia wide field dataset. This method has two main assumptions: that f is an unbiased estimate of CPC, and that fixed values of α and k can be used across a variety of tree stands.

3.5.2. Royal National Park study site

The proposed method of using Eq. (8) to derive FPC from lidar fractional cover was tested across 12 sites with coincident star transects and airborne lidar data in the Royal National Park, just south of Sydney, NSW (Fig. 1). In April 2013 an airborne lidar survey was acquired over the area, which included woodland (*Eucalyptus spp.*), mallee-heath-woodland (*Banksia spp.* and *Eucalyptus spp.*), and forest (*Angophora spp.*, *Corymbia spp.* and *Eucalyptus spp.*). The survey was acquired with a Leica ALS50-II instrument, flying at a mean height above ground of 1828 m, with a laser footprint diameter on the ground of 0.4 m, a maximum scan angle from nadir of 15°, and a mean pulse density of 1.3 pulses/m^2. The lidar data was acquired, processed, classified and delivered as a discrete return point cloud in the lidar exchange format (LAS), before conversion to the Sorted Pulse Data (SPD) format (Bunting et al., 2013b). The height of each return above ground was calculated with natural neighbour interpolation using functions available in the SPDLib software (Bunting et al., 2013a).

Star transects were measured at 12 sites, selected to sample a wide range of FPC values. Field recorded FPC and CPC were calculated according to the method outlined previously. Lidar fractional cover (f) was calculated from 100 m diameter circular areas at each field site location. Although 12 sites are a small sample, they provide enough data to illustrate the potential of the method.

4. Results

4.1. Distributions of k and α

Across the sites the values of k as calculated from CPC and FPC values using Eq. (10) ranged from 0.07-5.84, with a median value of 1.15 (Fig. 2A). The distribution is clearly positively skewed, with the 2.5th percentile (0.27) much closer to the median than the 97.5th percentile (3.81). As k increases, FPC increases towards the same value as CPC, while as k decreases FPC decreases for any given value of CPC. The parameter k is directly related to LAI, $G(0)$ and $\Omega(0)$, and inversely related to tree density (λ_c) and mean crown area (πr_c^2). For example, for a fixed value of CPC, if LAI increases so too does k and FPC. If the foliage is more horizontally distributed, $G(0)$ will be greater and k and FPC will increase. If the foliage clumping factor is greater than one, the foliage is regularly distributed, and k and FPC increase, while as the foliage clumping factor approaches zero the foliage becomes more aggregated into clumps and k and FPC decrease (Chen et al., 2005). If CPC is fixed but tree density is increased or mean crown area is increased (through increasing the area of crown overlap), then k and FPC must decrease.

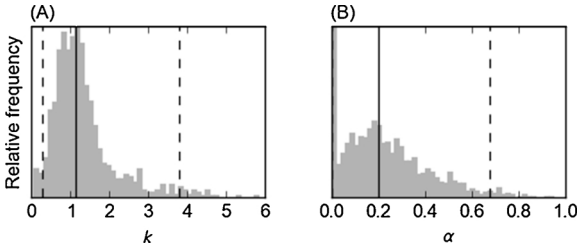

Fig. 2. (A) Histogram of k values calculated from field measurements using Eq. (10), showing the median value (1.15) as the solid line, and the 2.5th percentile (0.27) and 97.5th percentile (3.81) as dashed lines. The empirical parameter k is a function of several tree stand parameters (Eqs. (7) and (8)). (B) Histogram of αvalues calculated from field measurements using Eq. (4), showing the median value (0.20) as the solid line, and the 2.5th percentile (0.00) and 97.5th percentile (0.68) as dashed lines. The variable α is the proportion of woody elements to all canopy elements.

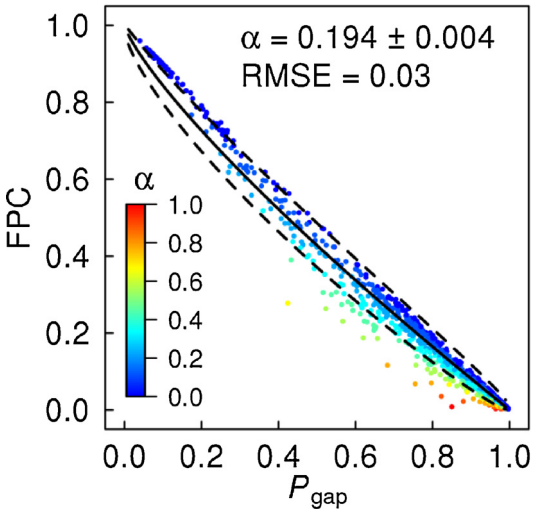

Fig. 3. The relationship between field measured P_{gap} and foliage projective cover (FPC) determined by Eq. (3) and α (the proportion of woody elements to all canopy elements). Non-linear weighted least-squares regression determined the best fit for Eq. (3) was with an α value of 0.194, which had a standard error of 0.004, and achieved a root mean square error (RMSE) of 0.03. The best-fit model is shown (solid line) with exact binomial 95% confidence intervals (dashed lines) calculated by propagating the standard error in α.

The distribution of α as calculated from FPC and P_{gap} using Eq. (4) ranged from 0.000.95, with a median value of 0.20 (Fig. 2B). The distribution is positively skewed, although large values of α were only observed for sites where FPC was low. For example, of the 113 sites where FPC was greater than 0.5, the maximum α was only 0.29. Conversely, the 295 sites where α was greater than 0.3 had a maximum FPC of only 0.44. As there is greater uncertainty in α when FPC is low, it is possible that the positive tail in its distribution is mostly a result of the sampling involved in the star transect method.

4.2. Predicting FPC from P_{gap}

The relationship between P_{gap}, FPC and α, described by Eq. (3), clearly fitted the observed site measurements very well (Fig. 3). Predicting FPC from all P_{gap} site measurements with Eq. (3) achieved a root mean square error (RMSE) of only 0.03 (3%). This model used an α value of 0.194, which is very close to the median value across all sites (Fig. 2B). When the median value of 0.2 was used, the RMSE was larger but still only 0.03 when measured at two decimal places. Propagating the very low standard error in α (0.004) through the model gives narrow 95% confidence intervals (Fig. 3), in large part due to the number and distribution of site values sampled (Fig. 2B). Sites that plot away from the model are those whose α calculated with Eq. (4) was large. These are all sites with low FPC, which have greater uncertainty in α due to a smaller sample of the canopy inherent in the star transect method.

4.3. Predicting FPC from CPC and vice versa

The models described by Eqs. (8) and (9) were fitted to the site data by fixing α at the best-fit value of 0.194, and using non-linear regression to solve for the best fit values of k (Fig. 4). When modelling FPC from CPC the best fit value of k was 0.98, which achieved a RMSE of 0.05

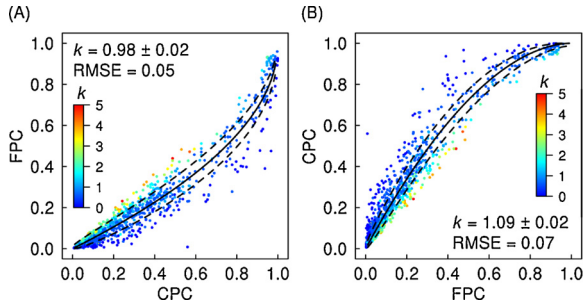

Fig. 4. The relationship between site measurements of FPC, CPC and k using non-linear weighted least-squares regression. (A) Modelling FPC from CPC using Eq. (8), the best fit value of k was 0.98, which had a standard error of 0.02 and achieved a root mean square error (RMSE) of 0.05. (B) Modelling CPC from FPC using Eq. (9), the best fit value of k was 1.09, which had a standard error of 0.02 and achieved an RMSE of 0.07. All models used the best fit α value of 0.194 (Fig. 3). The best-fit models are shown (solid line) with exact binomial 95% confidence intervals calculated by propagating the standard error in k.

(5%). Alternatively, when modelling CPC from FPC the best fit value of k and the RMSE were slightly larger at 1.09 and 0.07 (7%) respectively. The models appear to fit the data very well, following a near linear fit for low values of FPC and CPC before curving significantly (Fig. 4). The RMSE values are similar to that expected for the field measurements themselves. The low standard error in the fitted values of k, and the narrow confidence intervals show that the model is well constrained. When values for α and k are rounded to 0.2 and 1.0 respectively, the RMSE of the models remains the same. One site plots well beyond the model, with an FPC of 0.01 and CPC of 0.56. This site was measured after a fire had removed nearly all the foliage.

4.4. The influence of climate on α and k

The climatic conditions at each site do not correlate greatly with the values of k or α and offer little in the way of restricting the prediction of values (Fig. 5). In general, sites with greater mean annual rainfall have lower α, and sites with greater α have lower rainfall. For example, the 99 sites that have rainfall greater than 1500 mm have a mean and standard deviation α of 0.14 ± 0.14, compared to the overall mean and standard deviation of 0.23 ± 0.18. The 40 sites that have α greater than 0.6 have a mean and standard deviation rainfall of 449 ± 198 mm, compared to the overall mean and standard deviation of 706 ± 411 mm. Temperature and the drought indices ($SPEI_6$ and $SPEI_{24}$) have even weaker correlations with k or α (Fig. 5).

When the sites are grouped into different regions, there are some differences in the regional distributions of k and its median value (Fig. 6). The most tropical region in the north of the Northern Territory (NT north) has the largest median k (1.27), while the north of Queensland (QLD north) also has a high median k (1.24). Arid and more temperate regions such as NT south, QLD south, Western Australia (WA) and NSW have lower median k values. Larger mean values of k in the Australian tropics could be related to any of the variables that k is dependent on. It is possible that Australian trees in the tropics have a greater mean LAI when compared to those in arid and temperate areas. It may be that trees in the tropics have a greater mean $G(0)$ due to more horizontally distributed foliage, and/or greater mean $\Omega(0)$ due to more regularly distributed foliage. They may also have lower mean tree density and/or lower mean crown area, due to less overlapping crowns.

Although predicting k from climatic variables does not appear possible, there do appear to be some differences in the distribution of k values in different regions. Despite these differences, all regions with more than 15 sites have the overall median of 1.15 within their quartile range. Also, the minor regional differences do not result in regional model error being overly skewed when FPC is modelled from CPC using $k = 1.0$.

4.5. Calibrating airborne lidar metrics

The proposed method of deriving FPC from the lidar data performed well when compared across the 12 field sites (Fig. 7). When lidar fractional cover (f) was used as a proxy for CPC in Eq. (8) with $\alpha = 0.2$ and $k = 1.0$ the modelled FPC achieved an RMSE of 0.08 (Fig. 7B).

While the accuracy of the modelled FPC values for the 12 field sites shows the method has some promise, it does rely on two main assumptions that may not be true in all situations. Firstly, it was assumed that Eq. (8) with $\alpha = 0.2$ and $k = 1.0$ is appropriate to use across all tree stands. This assumption turned out to be relatively true for the 12 field sites; however, other sites or areas may require different values for α and/or k. Secondly, it was assumed that lidar fractional cover (f) is equivalent to CPC. This assumption also turned out to be relatively true for the 12 field sites (Fig. 7A). These two assumptions need to be tested across more field sites, encompassing a range of tree structures and lidar surveys, for the methods to be properly validated.

5. Discussion

5.1. Relating P_{gap}, CPC, FPC and LAI

Eq. (3) was found to describe the relationship between P_{gap} and FPC very well. The power model was controlled by α, the proportion of woody elements to all canopy elements, which was shown to have poor correlation with climate variables. When the median (0.20) or best fit α (0.19) values were used in Eq. (3) to model FPC from P_{gap}, the model achieved a very low RMSE (0.03). Furthermore, sites whose field measured FPC was significantly less than that predicted by the model all had FPC < 0.4, and were likely to have greater field measurement error. While the α value of 0.2 may not be applicable for any one site, it appears to be a very good fit when examining a collection of sites. On average, Australian tree stands have around 20% woody material in the canopy.

As the database used to explore the relationship between CPC and FPC did not include any measurements of LAI, $\Omega(0)$, $G(0)$, λ_c, or r_c, Eq. (7) could not be validated. The introduction of parameter k created the simpler Eq. (8), and allowed the relationship to be analysed, but it also created the problem of how to estimate suitable values for k. Exploration of possible relationships between k and several other variables (rainfall, temperature, and drought indices) did not reveal any strong correlations that might allow k to be predicted for different site conditions. It is assumed that k is a function of tree stand architecture, influenced by species, growth form, and previous disturbance events such as droughts, fires, or pests. These factors are likely influenced by climatic conditions, but climatic conditions alone are not enough to predict k.

Eqs. (5a), (5b), (5c) and other models developed by Nilson (1999) are usually applied to site measurements of $P_{gap}(\theta)$ made across a variety of zenith angles, along with other complementary measurements such as of stand density and crown radius (Nilson and Kuusk, 2004; Pisek et al., 2011). The site transect measurements used here were made at a single zenith angle of zero, and only allow the calculation of CPC and FPC, or the related canopy gap distributions (P_{gap}). We are not aware of similar data having been collected at other locations, meaning there is currently no scope to make meaningful comparisons between the Australian sites and data collected around the world.

5.2. Converting between CPC and FPC

The models for converting FPC and CPC give remarkably low RMSE values (0.05–0.07) when Eqs. (8) and (9) are used with fixed values of α and k. It should be noted that these errors are applicable to sufficiently large samples of tree stands, which appear to have consistent average values of α and k. These values may not be applicable to any one site,

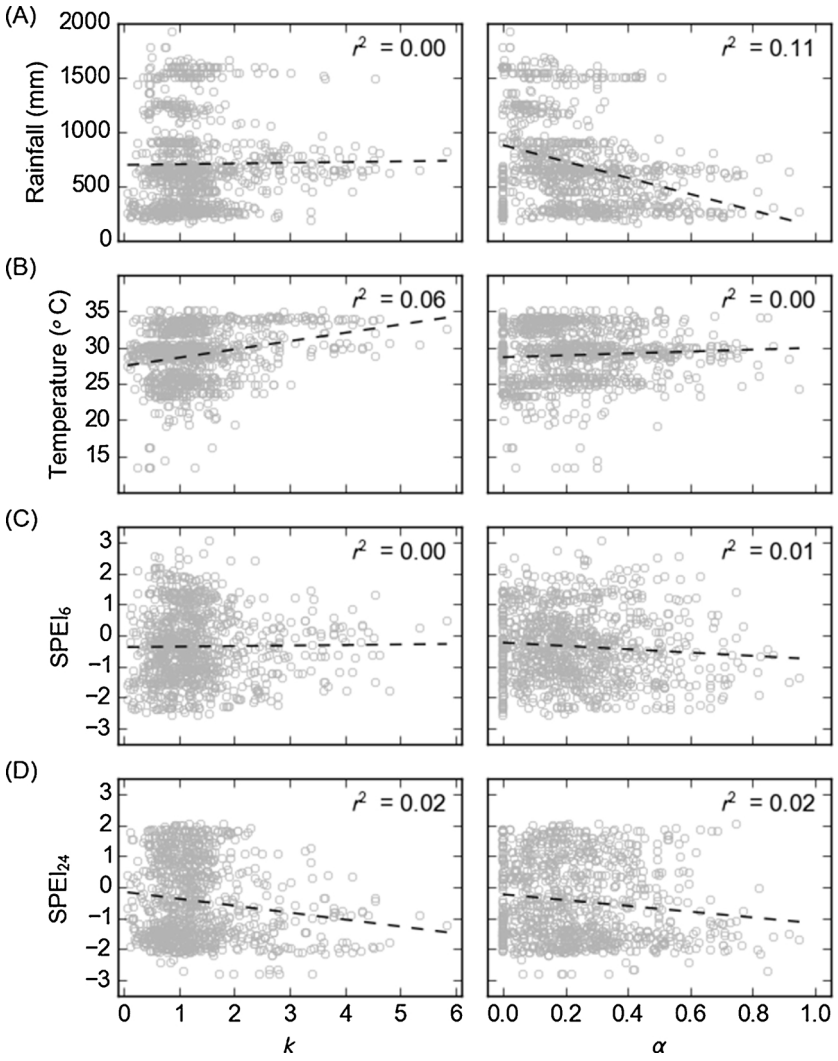

Fig. 5. The relationship between k, $\alpha$and four climate variables for each site: (A) mean annual precipitation; (B) mean daily maximum temperature; (C) the standardized precipitation and evaporation index (SPEI) over 6 months, and; (D) SPEI over 2 years. The dashed lines and correlation coefficient values (r^2) represent the relationship between plotted variables, calculated using ordinary least squares regression.

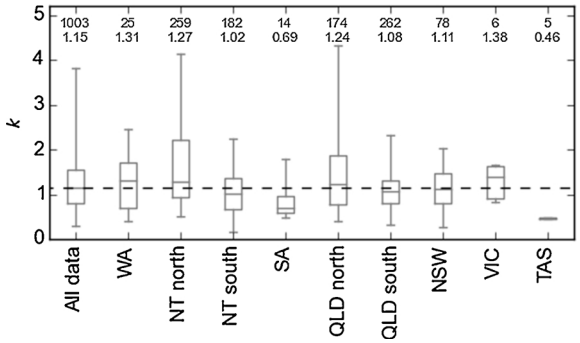

Fig. 6. Boxplot distributions of k values for sites from different regions of Australia, showing the median (middle line), quartile (box) and 95% confidence limits (whiskers), while the grey numbers show the number of sites and the median k value in each region. Regions were chosen based on Australia's states, whose names are given in full in Fig. 1.

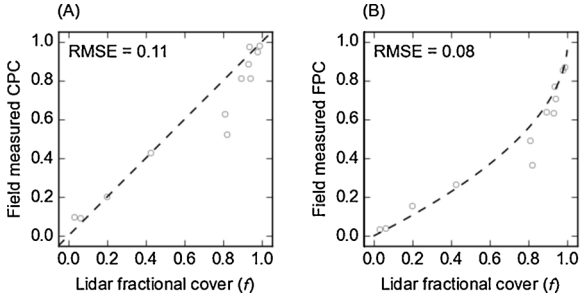

Fig. 7. (A) Lidar fractional cover (f) and field measured CPC for the 12 Royal National Park sites, where the dashed line is the 1:1 line from which the root mean square error (RMSE) was calculated. (B) Lidar fractional cover (f) and field measured FPC, where the dashed line and RMSE were calculated from Eq. (8) using $\alpha = 0.2$ and $k = 1.0$.

where the modelling error may be significantly larger.

Simplifying Eqs. (8) and (9) using the best fit values results in Eqs. (13) and (14), which are remarkably simple when compared to the original Eq. (7).

$$FPC = 1-(1-CPC)^{0.50} \quad (13)$$

$$CPC = 1-(1-FPC)^{1.86} \quad (14)$$

These equations facilitate the easy conversion between the two metrics for Australian tree stands, and the RMSE for the equations can be used as estimates of uncertainty in such conversions. This includes

metrics derived from remote sensing data, such as FPC derived from Landsat satellite imagery (Armston et al., 2009), from SPOT5 satellite imagery (Fisher et al., 2016) or airborne imagery (Staben et al., 2016). Converting these maps of FPC into maps of CPC then allows the classification of forest using the CPC threshold of 0.2 (Montreal Process Implementation Group for Australia and National Forest Inventory Steering Committee, 2013). Converting 0.2 CPC results in 0.11 FPC, which is very close to the value of 0.12 suggested by Henry et al. (2002). However, when the RMSE of the model (0.05) is taken into account, the modelled FPC has a 95% confidence interval of 0.01–0.20. Any maps created through this conversion need to be viewed with an understanding of this uncertainty.

5.3. Airborne lidar application

The method proposed to use the FPCCPC relationship in deriving FPC from airborne lidar data was demonstrated for the Royal National Park study site. It was able to derive FPC from lidar fractional cover with an RMSE of 0.08, which is very similar to previous studies that used field data to calibrate models of FPC (Armston et al., 2009; Ediriweera et al., 2013). The method required two main assumptions: that fixed values of α (0.2) and k (1.0) can be used across the study area, and; that lidar fractional cover is a direct estimate of CPC. Each assumption was found to be true when validated against the field data. It is not known however, how probable this is for other areas or lidar surveys. It may be that given a large sample of tree stands with a variety of species and structures, the median value of k will always be approximately 1.0. The fact that k was not found to have any correlation with climate or location across all the Australian field sites, supports this. Furthermore, while the median value of k was 1.15 the 95% bootstrapped confidence interval was only1.11-1.19, which is a very narrow range.

6. Conclusion

The work presented here explored the relationship between CPC and FPC across Australia, and has provided a method for converting between the two tree cover metrics. Developed from the research of Nilson (1999), Eq. (7) describes the relationship between CPC and FPC as a function of LAI, the foliage clumping factor at a zenith angle of zero ($\Omega(0)$), the foliage projection function at a zenith angle of zero ($G(0)$), tree stand density (λ_c), the mean crown radii (r_c), and the proportion of woody elements to all canopy elements (α). Simplifying this model by introducing the parameter k removed LAI, $\Omega(0)$, $G(0)$, λ_c and r_c and allowed the relationship described by Eqs. (8) and (9) to be investigated for a large database of coincident field measurements of FPC and CPC across Australia. Using the best-fit values of α and k, the equations were simplified even further into Eqs. (13) and (14), which can be used to derive FPC from CPC, and *vice versa*. These models achieved low RMSE (0.050.07) across the field data, even though they did not allow for known seasonal variations in tree and leaf structure, or any site specific conditions. Eqs. (13) and (14) offer a method of converting between the two tree cover metrics, which allows different mapping projects to be compared. The models also provide a method for deriving FPC from airborne lidar data, when field measurements of FPC are not available for calibration. Although the method appears to be promising, more research is required to investigate its stability across a variety of regional areas using data from different lidar systems.

Acknowledgments

Thanks to all who contributed to the collection of the field data and to the Bureau of Meteorology for making rainfall and temperature grids of Australia freely available. Thanks also to the anonymous reviewers who provided new insights into the research, which greatly enhanced the paper.

References

Armston, J., Scarth, P., Disney, M., Phinn, S., Lucas, R., Bunting, P., Goodwin, N., 2012. Estimation of foliage projective cover, leaf area index and crown cover from airborne lidar across multiple bioregions in eastern Australia. In: Proceedings of the XXII Congress of the International Society for Photogrammetry and Remote Sensing. 25 August - 1 September 2012., Melbourne.

Armston, J.D., Denham, R.J., Danaher, T.J., Scarth, P.F., Moffiet, T.N., 2009. Prediction and validation of foliage projective cover from Landsat-5 TM and Landsat-7 ETM + + imagery. J. Appl. Remote Sens. 3 (1), 033540.

Bates, D.M., Watts, D.G., 1988. Nonlinear Regression Analysis and Its Applications. Wiley Series in Probability and Mathematical Statistics. Wiley New York.

Bowman, D.M.J.S., Prior, L.D., 2005. TURNER REVIEW no. 10. Why do evergreen trees dominate the Australian seasonal tropics? Aust. J. Bot. 53 (5), 379.

Bunting, P., Armston, J., Clewley, D., Lucas, R.M., 2013a. Sorted pulse data (SPD) library—part II: a processing framework for LiDAR data from pulsed laser systems in terrestrial environments. Comput. Geosci. 56, 207–215.

Bunting, P., Armston, J., Lucas, R.M., Clewley, D., 2013b. Sorted pulse data (SPD) library. Part I: a generic file format for LiDAR data from pulsed laser systems in terrestrial environments. Comput. Geosci. 56, 197–206.

Bureau of Meteorology, 2015. Maps of Recent and Past Conditions. , last accessed on 28/10/2015. http://www.bom.gov.au/climate/maps.

Campbell, G.S., 1990. Derivation of an angle density function for canopies with ellipsoidal leaf angle distributions. Agric. Forest Meteorol. 49 (3), 173–176.

Chen, J.M., Black, T.A., 1992. Defining leaf area index for non-flat leaves. Plant Cell Environ. 15, 421–429.

Chen, J.M., Cihlar, J., 1996. Retrieving leaf Area index of boreal conifer forests using landsat TM images. Remote Sens. Environ. 55, 153–162.

Chen, J.M., Menges, C.H., Leblanc, S.G., 2005. Global mapping of foliage clumping index using multi-angular satellite data. Remote Sens. Environ. 97 (4), 447–457.

Chen, J.M., Rich, P.M., Gower, S.T., Norman, J.M., Plummer, S., 1997. Leaf area index of boreal forests: theory, techniques, and measurements. J. Geophys. Res. 102 (D24), 29429.

Chen, X., Vierling, L., Rowell, E., DeFelice, T., 2004. Using lidar and effective LAI data to evaluate IKONOS and landsat 7 ETM + + vegetation cover estimates in a ponderosa pine forest. Remote Sens. Environ. 91 (1), 14–26.

Danaher, T., Scarth, P., Armston, J., Collett, L., Kitchen, J., Gillingham, S., 2010. Remote sensing of tree-grass systems: the Eastern Australian Woodlands. In: Hill, M.J., Hanan, N.P. (Eds.), Ecosystem Function in Savannas: Measurement and Modeling at Landscape to Global Scales. CRC Press, Boca Raton, pp. 175–194.

Ediriweera, S., Pathirana, S., Danaher, T., Nichols, D., Moffiet, T., 2013. Evaluation of different topographic corrections for landsat TM data by prediction of foliage projective cover (FPC) in topographically complex landscapes. Remote Sens. 5 (12), 6767–6789.

Falster, D.S., Westoby, M., 2003. Leaf size and angle vary widely across species: what consequences for light interception? New Phytologist 158 (3), 509–525.

FAO, 2012. FRA 2015 Terms and Definitions, Forest Resources and Assessment Working Paper 180. Food and Agriculture Organization of the United Nations, Rome, pp. 36.

Fensham, R.J., Fairfax, R.J., Choy, S.J.L., Cavallaro, P.C., 2003. Modelling trends in woody vegetation structure in semi-arid Australia as determined from aerial photography. J. Environ. Manage. 68 (4), 421–436.

Fisher, A., Day, M., Gill, T., Roff, A., Danaher, T., Flood, N., 2016. Large-area, high-resolution tree cover mapping with multi-temporal SPOT5 imagery, New South Wales, Australia. Remote Sens. 8 (6), 515.

Gill, T.K., Phinn, S.R., Armston, J.D., Pailthorpe, B.A., 2009. Estimating tree-cover change in Australia: challenges of using the MODIS vegetation index product. Int. J. Remote Sens. 30 (6), 1547–1565.

Gonsamo, A., D'odorico, P., Pellikka, P., 2013. Measuring fractional forest canopy element cover and openness - definitions and methodologies revisited. Oikos 122 (9), 1283–1291.

Henry, B., Danaher, T., McKeon, G., Burrows, W., 2002. A review of the potential role of greenhouse gas abatement in native vegetation management in Queensland's rangelands. Rangel. J. 42 (1), 112–132.

Johansson, T., 1985. Estimating canopy density by the vertical tube method. For. Ecol. Manage. 11, 139–144.

Jonckheere, I., Fleck, S., Nackaerts, K., Muys, B., Coppin, P., Weiss, M., Baret, F., 2004. Review of methods for in situ leaf area index determination. Agric. For. Meteorol. 121 (1-2), 19–35.

Jones, D.A., Wang, W., Fawcett, R., 2009. High-quality spatial climate data-sets for Australia. Aust. Meteorol. Oceanogr. J. 58, 233–248.

King, D.A., 1997. The functional significance of leaf angle in eucalyptus. Aust. J. Bot. 45 (4), 619–639.

Korhonen, L., Korpela, I., Heiskanen, J., Maltamo, M., 2011. Airborne discrete-return LIDAR data in the estimation of vertical canopy cover, angular canopy closure and leaf area index. Remote Sens. Environ. 115 (4), 1065–1080.

Lovell, J.L., Jupp, D.L.B., Culvenor, D.S., Coops, N.C., 2003. Using airborne and ground-based ranging lidar to measure canopy structure in Australian forests. Can. J. Remote Sens. 29 (5), 607–622.

Lucas, R., Cronin, N., Moghaddam, M., Lee, A., Armston, J., Bunting, P., Witte, C., 2006. Integration of radar and landsat-derived foliage projected cover for woody regrowth mapping, Queensland, Australia. Remote Sens. Environ. 100 (3), 388–406.

Montreal Process Implementation Group for Australia and National Forest Inventory Steering Committee, 2013. Australia's State of the Forests Report 2013. ABARES, Canberra.

Muir, J., Schmidt, M., Tindall, D., Trvithick, R., Scarth, P., Stewart, J., 2011. Field

Measurement of Fractional Ground Cover: a Technical Handbook Supporting Ground Cover Monitoring for Australia. Prepared by the Queensland Department of Environment and Resource Management for the Australian Bureau of Agricultural and Resource Economics and Sciences, Canberra.
Nilson, T., 1971. A theoretical analysis of the frequency of gaps in plant stands. Agric. Meteorol. 8, 25–38.
Nilson, T., 1999. Inversion of gap frequency data in forest stands. Agric. For. Meteorol. 98–99, 437–448.
Nilson, T., Kuusk, A., 2004. Improved algorithm for estimating canopy indices from gap fraction data in forest canopies. Agric. Forest Meteorol. 124 (3-4), 157–169.
Pisek, J., Lang, M., Nilson, T., Korhonen, L., Karu, H., 2011. Comparison of methods for measuring gap size distribution and canopy nonrandomness at Järvselja RAMI (RAdiation transfer model intercomparison) test sites. Agric. For. Meteorol. 151 (3), 365–377.
Queensland Department of Science Information Technology Innovation and the Arts, 2014. Land Cover Change in Queensland 2011–12: a Statewide Landcover and Trees Study (SLATS) Report. DSITIA, Brisbane.
R Development Core Team, 2016. R: A Language and Environment for Statistical Computing. R Foundation for Statistical Computing, Vienna.
Scarth, P., Armston, J., Danaher, T., 2008. On the relationship between crown cover, foliage projective cover and leaf area index. In: Proceedings of the 14th Australian Remote Sensing and Photogrammetry Conference. 29 September – 3 October 2008, Darwin.
Scarth, P., Phinn, S., 2000. Determining forest structural attributes using an inverted geometric-optical model in mixed eucalypt forests, Southeast Queensland, Australia. Remote Sens. Environ. 71 (2), 141–157.
Schliemann, S.A., Bockheim, J.G., 2011. Methods for studying treefall gaps: a review. For. Ecol. Manage. 261 (7), 1143–1151.
Simioni, G., Gignoux, J., Le Roux, X., 2003. Tree layer spatial structure can affect savanna production and water budget: results of a 3-D model. Ecology 84 (7), 1879–1894.
Specht, R.L., 1970. Vegetation. In: Leeper, G.W. (Ed.), The Australian Environment. CSIRO in association with Melbourne University Press, Melbourne, pp. 44–67.
Specht, R.L., 1983. Foliage projective covers of overstory and understory strata of mature vegetation in Australia. Austral Ecol. 8, 433–439.
Specht, R.L., Specht, A., 1999. . Australian Plant Communities: Dynamics of Structure, Growth and Biodiversity. Oxford University Press, Melbourne, Australia, pp. 492.
Staben, G.W., Lucieer, A., Evans, K.G., Scarth, P., Cook, G.D., 2016. Obtaining biophysical measurements of woody vegetation from high resolution digital aerial photography in tropical and arid environments: Northern Territory, Australia. Int. J. Appl. Earth Obs. Geoinf. 52, 204–220.
Thornthwaite, C.W., 1948. An approach toward a rational classification of climate. Geogr. Rev. 38, 55–94.
Trevithick, R., 2017. SLATS Star Transect Data. AusCover Remote Sesing Data Facility, Terrestrial Ecosystem Research Network. last accessed on 3/10/2017. http://data.auscover.org.au/Portal2/.
Trevithick, R., Muir, J., Denham, R., 2012. The effect of observer experience levels on the variability of fractional ground cover reference data. In: International Archives of the Photogrammetry, Remote Sensing and Spatial Information Sciences. ISPRS Congress, Melbourne, Australia.
Vepakomma, U., St-Onge, B., Kneeshaw, D., 2008. Spatially explicit characterization of boreal forest gap dynamics using multi-temporal lidar data. Remote Sens. Environ. 112 (5), 2326–2340.
Vicente-Serrano, S.M., Beguería, S., López-Moreno, J.I., 2010. A multiscalar drought index sensitive to global warming: the standardized precipitation evapotranspiration index. J. Clim. 23 (7), 1696–1718.
Walker, J., Hopkins, M.S., 1990. Australian soil and land survey : field handbook. In: McDonald, R.C., R.F, Isbell, Speight, J.G., Walker, J., Hopkins, M.S. (Eds.), Australian Soil and Land Survey : Field Handbook. CSIRO, Canberra, pp. 190.
Wulder, M.A., White, J.C., Nelson, R.F., Næsset, E., Ørka, H.O., Coops, N.C., Hilker, T., Bater, C.W., Gobakken, T., 2012. Lidar sampling for large-area forest characterization: a review. Remote Sens. Environ. 121, 196–209.